Diagn Interv Radiol 2021; 27:469-475

CHEST IMAGING

ORIGINAL ARTICLE

Spin-echo and diffusion-weighted MRI in differentiation between progressive massive fibrosis and lung cancer

Serkan Guneyli
Meltem Tor
Hur Hassoy
Murat Serhat Aygun
Emre Altinmakas
Susamber Dik Altintas
Recep Savas

PURPOSE
We aimed to investigate the value of magnetic resonance imaging (MRI)-based parameters in differentiating between progressive massive fibrosis (PMF) and lung cancer.

METHODS
This retrospective study included 60 male patients (mean age, 67.0±9.0 years) with a history of more than 10 years working in underground coal mines who underwent 1.5 T MRI of thorax due to a lung nodule/mass suspicious for lung cancer on computed tomography. Thirty patients had PMF, and the remaining ones had lung cancer diagnosed histopathologically. The sequences were as follows: coronal single-shot turbo spin echo (SSH-TSE), axial T1- and T2-weighted spin-echo (SE), balanced turbo field echo, T1-weighted high-resolution isotropic volume excitation, free-breathing and respiratory triggered diffusion-weighted imaging (DWI). The patients' demographics, lesion sizes, and MRI-derived parameters were compared between the patients with PMF and lung cancer.

RESULTS
Apparent diffusion coefficient (ADC) values of DWI and respiratory triggered DWI, signal intensities on T1-weighted SE, T2-weighted SE, and SSH-TSE imaging were found to be significantly different between the groups ($p < 0.001$, for all comparisons). Median ADC values of free-breathing DWI in patients with PMF and cancer were 1.25 (0.93–2.60) and 0.76 (0.53–1.00) ($\times 10^{-3}$ mm^2/s), respectively. Most PMF lesions were predominantly iso- or hypointense on T1-weighted SE, T2-weighted SE, and SSH-TSE, while most malignant ones predominantly showed high signal intensity on these sequences.

CONCLUSION
MRI study including SE imaging, specially T1-weighted SE imaging and ADC values of DWI can help to distinguish PMF from lung cancer.

Pneumoconiosis, defined as the accumulation of inhaled particles is relatively common in industrial areas (1). Coal worker's pneumoconiosis, silicosis, and asbestosis are the most common forms of pneumoconiosis (2). Progressive massive fibrosis (PMF) of the lung is defined as a combination of anthracosilicotic nodules and connective tissue, and it may be seen in the chronic stage of pneumoconiosis (1).

The imaging features of PMF on chest radiography and computed tomography (CT) have been well investigated (3, 4). The main characteristic finding of PMF on CT is an irregular nodule or mass with or without calcification, located mostly in the upper and middle lung zones (5). However, it is occasionally difficult to distinguish PMF from lung cancer due to a similar appearance on these imaging modalities as well as similar clinical presentation. The differentiation is especially difficult, when PMF lesion appears as a mass or mass-like lesion and grows in size during the follow-up. Additionally, lung cancer may be seen together with underlying PMF lesion. 18F-fluoro-2-deoxy-D-glucose positron emission tomography/CT (^{18}F-FDG PET/CT) can be used in differentiation between PMF and lung cancer but it may not be helpful in some cases (6).

Magnetic resonance imaging (MRI) with high conrast resolution and additional diignostic facility tools may be helpful in terms of avoiding biopsy and its possible complications

From the Department of Radiology (S.G ✉ *drserkanguneyli@gmail.com*, M.S.A., E.A.), Koc University, Istanbul, Turkey; Department of Pulmonology (M.T., S.D.A.), Bulent Ecevit University, Zonguldak, Turkey; Departments of Public Health (H.H.) and Radiology (R.S.), Ege University, Izmir, Turkey.

Received 13 May 2020; revision requested 15 June 2020; last revision received 1 July 2020; accepted 12 July 2020.

Published online 22 June 2021.

DOI 10.5152/dir.2021.20344

You may cite this article as: Guneyli S, Tor M, Hassoy H, et al. Spin-echo and diffusion-weighted MRI in differentiation between progressive massive fibrosis and lung cancer. Diagn Interv Radiol 2021; 27:469-475

in the differentiation between PMF and lung cancer (7, 8). A low signal intensity (SI) on T2-weighted MRI and a gradual increase in SI in a dynamic MRI study are the reported, characteristic MRI findings of PMF (9, 10). However, the use of several MRI sequences has not yet been fully explored for the differentiation between PMF and lung cancer. In addition to the SI changes, assessment of quantitative MRI parameters could also be helpful in the differentiation of these entities. The purpose of this study was to investigate the value of MRI-based parameters in differentiating between PMF and lung cancer.

Methods

Patient selection

This retrospective study was conducted with an Institutional Review Board-approved waiver of informed consent (Decision number of ethics committee approval: 19-7T/87). We searched the patient records in our institution to identify patients who underwent unenhanced MRI of thorax. In our institution, MRI has been increasingly performed in patients whose lesions could not be differentiated using CT or ^{18}F-FDG PET/CT. In all, 67 male patients with a working history of more than 10 years in coal mines who underwent MRI of thorax due to a lung nodule/mass suspicious for lung cancer on CT between June 2018 and October 2019 were identified. Patients with poor image quality (n=2), a nodule/mass containing marked, amorphous calcifications (n=2), missing histopathological results (n=1), and patients who worked less than 10 years in underground coal mines (n=2) were excluded, leaving 60 patients with a mean age of 67.0±9.0 years, who were histologically diagnosed with PMF or lung cancer, included in this study.

The age, duration of active working history in underground coal mines, duration and amount of smoking history of the patient were regarded as numerical parameters. Age, duration of work history in the coal mines, and lesion size were noted from institutional records. The amount of smoking which was calculated by multiplying the duration of smoking years and the package of cigarettes was also noted. In case there were more than one lung lesion, the most suspicious lesion for cancer was histologically evaluated in each patient. The lesion or part of the lesion most suspicious for cancer was determined based on high SI on diffusion-weighted imaging (DWI) and low SI on apparent diffusion coefficient (ADC) map and these lesions were biopsied under CT guidance. Thirty patients had a diagnosis of PMF, while the remaining 30 patients had a diagnosis of lung cancer. The histopathological subtypes of cancer were also noted. The patients did not have interstitial fibrosis on CT.

Main points

- Progressive massive fibrosis (PMF) can occur in patients who chronically inhale industrial particles such as coal dust, silica, and asbestos. PMF lesions may progress and mimic lung cancer.
- CT and 18F-FDG PET/CT may be unable to distinguish PMF from lung cancer in some patients.
- ADC values of diffusion-weighted MRI quantitatively and the signal intensities on MRI sequences, especially T1-weighted SE, qualitatively were found to be strong predictors in differentiation between PMF and lung cancer.
- ADC values of PMF lesions were found to be higher compared to those obtained from cancer lesions, and PMF lesions were predominantly seen as iso- or hypointense on T1-, T2-weighted SE, and SSH-TSE due to the signal intensity of fibrosis.
- Multiparametric MRI examination is a noninvasive, tolerable, nonionizing method which may increase the diagnostic ability in differentiation of PMF from lung cancer and play a role in targeting possible biopsy locations due to its detailed visualization of the lesion structure.

Image acquisition

All MRI scans were obtained with a body coil by using a 1.5 T MRI scanner (Ingenia, Philips Healthcare). The entire thoracic cavity was scanned, and the following sequences were obtained: axial T1- and T2-weighted spin-echo (SE), coronal single-shot turbo SE (SSH-TSE), balanced turbo field echo (BTFE), T1-weighted high-resolution isotropic volume excitation (THRIVE), free-breathing DWI, and respiratory-triggered DWI (rt-DWI). All sequences were obtained under free-breathing technique, and rt technique (respiratory belt) was used in all sequences except for free-breathing DWI. The total image acquisition time was 25 minutes. T2-weighted SE imaging parameters were as follows: repetition time/echo time (TR/TE), 2690–5700/50–110 ms; matrix, 360×240; section thickness, 5.65 mm; intersection gap, 0.85 mm; field of view, 32–36 cm. T1-weighted SE imaging parameters were as follows: TR/TE, 170–607 / 2.4–9 ms; matrix, 248×160; section thickness, 6 mm; intersection gap, 2 mm; field of view, 27–34 cm. DWI was obtained by a single-shot SE echoplanar imaging sequence with a TR/TE, 1840–4400/56–84 ms; matrix, 120×104; section thickness, 6 mm; field of view, 36–40 cm; diffusion-encoding gradient pulses applied in the x, y, and z axes with b= 1000 s/mm^2.

Image analysis

The images were reviewed on a special commercial workstation and we obtained T1- and T2-weighted SE sequences in our study. A radiologist (S.G.) with 15 years of experience in thorax MRI reviewed the images of the patients blinded to the histopathological diagnoses. For the purpose of assessing interobserver agreement, another radiologist (M.S.A.) with 14 years of experience in thorax MRI was required to evaluate the below parameters separately and independently.

The size of the lesion and the ADC values of free-breathing DWI and rt-DWI were regarded as numerical parameters. Since cancers generally show hypercellularity and thus diffusion restriction, solid parts without calcification, most hyperintense parts on DWI, and most hypointense parts (compared to the muscle SI) on ADC image were considered as most suspicious parts of the lesion for a possible neoplasia, and ADC values of the lesions were assessed from these parts. An average ADC value for each lesion was calculated from 3 different region-of-interest (ROI) measurements on the ADC maps of both DWI and rt-DWI, and a ROI of 1.5 cm^2 was used. The SIs on T1- and T2-weighted SE, SSH-TSE, BTFE, and THRIVE were regarded as categorical parameters. Based on these MRI sequences, the patients were classified into 2 groups as those with predominantly iso-/hypointense lesions and those with predominantly hyperintense lesions compared to the muscle SI.

Statistical analysis

Student t test was used for the comparisons of age and amount of smoking history, while Mann–Whitney U test was used for the comparisons of the other numerical variables between the PMF and cancer groups. Categorical parameters were compared using Pearson chi-square test. MRI parameters were also compared between patients with different subtypes of cancer. Pearson correlation coefficient (r) was calculated between the ADC values of DWI and rt-DWI. Interobserver agreement between the two radiologists in the

Table 1. Comparison of patient characteristics and ADC values between PMF and lung cancer groups

	PMF	Lung cancer	*p*
Age (years), mean±SD	66.3±9.4	65.9±8.7	0.854
Duration of working in coal mines (years), median (range)	21 (10–30)	16 (11–30)	0.033*
Amount of smoking (years × packages of cigarettes), mean±SD	18.1±20.9	33.1±16.5	0.083
Largest diameter of lesion (mm), median (range)	44 (16–90)	41 (17–120)	0.796
ADC of DWI ($\times 10^{-3}$ mm^2/s), median (range)	1.25 (0.93–2.60)	0.76 (0.53–1.00)	<0.001*
ADC of rt-DWI ($\times 10^{-3}$ mm^2/s), median (range)	1.39 (0.98–2.90)	0.72 (0.44–1.04)	<0.001*

ADC, apparent diffusion coefficient; PMF, progressive massive fibrosis; SD, standard deviation; DWI, diffusion-weighted imaging; rt-DWI, respiratory triggered diffusion-weighted imaging.
*Statistical significance was considered at $p < 0.05$.

Table 2. Frequency and percentage of patients with PMF and lung cancer lesions appearing predominantly as iso- or hypointense on MRI sequences

	PMF, n (%)	Lung cancer, n (%)	*p*
T1-weighted SE	30 (100%)	2 (6.6%)	< 0.001*
T2-weighted SE	27 (90%)	6 (20%)	< 0.001*
THRIVE	6 (20%)	5 (16.6%)	0.739
BTFE	25 (83.3%)	24 (80%)	1.000
SSH-TSE	21 (70%)	4 (13.3%)	< 0.001*

PMF, progressive massive fibrosis; MRI, magnetic resonance imaging; SE, spin-echo; SSH-TSE, single-shot turbo spin-echo; BTFE, balanced turbo field echo; THRIVE, T1-weighted high-resolution isotropic volume excitation.
*Statistical significance was considered at $p < 0.05$.

assessment of categorical parameters was evaluated using Cohen's Kappa test. One sample t test, visual inspection of Bland–Altman plot, and linear regression were used to determine the level of agreement of two observers' measurements of ADC values. The level of statistical significance was set at $p < 0.05$.

Results

The mean and median values of numerical parameters and their comparisons between the groups are presented in Table 1. The medians of largest diameter of lesions in PMF and cancer groups were 44 mm (16–90 mm) and 41 mm (17–120 mm), respectively. ADC values of DWI ($p < 0.001$) and rt-DWI ($p < 0.001$) were significantly elevated in PMF patients compared with the cancer patients. Median ADC values of DWI and rt-DWI in cancer group were 0.76 $\times 10^{-3}$ mm^2/s (0.53–1.00 $\times 10^{-3}$ mm^2/s) and 0.72 $\times 10^{-3}$ mm^2/s (0.44–1.04 $\times 10^{-3}$ mm^2/s), respectively. Median ADC values of DWI and rt-DWI in PMF group were 1.25 $\times 10^{-3}$ mm^2/s (0.93–2.60 $\times 10^{-3}$ mm^2/s) and 1.39 $\times 10^{-3}$ mm^2/s (0.98–2.90 $\times 10^{-3}$ mm^2/s), respectively. Additionally, the duration of working history in coal mines was significantly higher in PMF group ($p = 0.014$). Age, duration and amount of smoking and the size of the lesion were not significantly different between the disease groups.

The frequency of PMF and cancer lesions appearing predominantly as iso- or hypointense on MRI and the comparison of categorical parameters between the groups are presented in Table 2. The SIs on T1-weighted SE ($p < 0.001$), T2-weighted SE ($p < 0.001$), and SSH-TSE ($p < 0.001$) were significantly different between the PMF and cancer groups. PMF lesions were predominantly seen as iso- or hypointense on T1 and T2-weighted SE and SSH-TSE (Figs. 1 and 2), while malignant lesions predominantly showed hyperintense signals (Fig. 3). Other categorical parameters did not show significant correlation.

The frequency of patients with different subtypes of cancers were as follows: 15 patients had squamous cell carcinoma, 12 patients had adenocarcinoma, and 3 patients had small cell lung cancer. In the comparison between these subtypes, there was no significant correlation of numerical and categorical MRI parameters.

In correlation between the ADC values of DWI and rt-DWI, there was a significant and very strong positive correlation ($r = 0.960$, $p < 0.001$). There was no significant difference in the interobserver agreement between the two radiologists in terms of categorical parameters. The Kappa coefficients of SIs on T1- and T2-weighted SE, SSH-TSE, BTFE, and THRIVE were 1.000, 0.966, 0.942, 0.848, and 1.000, respectively. The interobserver agreement of all categorical parameters was $p < 0.001$. There was no significant difference in the interobserver agreement between the two radiologists in terms of ADC values in comparison using one sample t test, linear regression, and visual inspection of Bland Altman Plot (Fig. 4). For the interobserver agreement of ADC values, *p* value was greater than 0.05 for one sample t test. In linear regression, the interobserver agreement parameters for ADC values of DWI were as follows: adjusted $R^2 = 0.137$, β-coefficient (unstandardized) = 0.097, standard error = 0.030, $p = 0.002$, standardized β-coefficient = 0.390, ICC values (95% confidence interval) = 0.15–0.37. The interobserver agreement parameters for ADC values of rt-DWI were as follows: adjusted $R^2 = 0.106$, β-coefficient (unstandardized) = 0.127, SE= 0.044, $p = 0.007$, standardized β-coefficient = 0.347, ICC values (95% confidence interval) = 0.21–0.36. These results pointed that fair to excellent agreement could be expected between any pair of two radiologists.

Discussion

PMF is a histopathological diagnosis that can occur in patients who chronically inhale industrial particles such as coal dust, silica, asbestos; progression of PMF lesions makes its differentiation from lung cancer more difficult (1, 4, 5). It is important to rule out lung cancer in the management of patients with PMF. We performed this study to better understand the role of MRI in differentiation between PMF and lung cancer. Our results show that several MRI-derived parameters (ADC values on DWI and rt-DWI and the SI values on T1-weighted SE, T2-weighted SE, and SSH-TSE) demonstrated significant difference between PMF and cancer groups. In our study, higher ADC values and more hypointense appearances on SE MRI, especially T1-weighted SE MRI were found in patients with PMF compared with the patients with lung cancer.

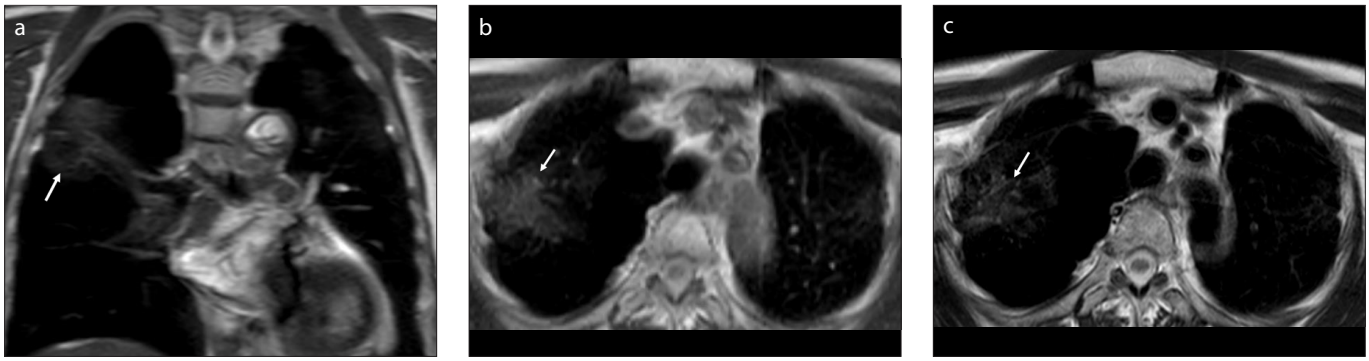

Figure 1. a–e. A 70-year-old man with PMF who worked in coal mines for 16 years. Coronal SSH-TSE image **(a)** shows an ill-defined, mildly hypointense mass *(arrow)* in the right lung. The lesion is isointense on axial T1-weighted SE image (**b,** *arrow*), hypointense on axial T2-weighted SE image (**c,** *arrow*), hypointense on BTFE image (**d,** *arrow*), and hyperintense on THRIVE image (**e,** *arrow*).

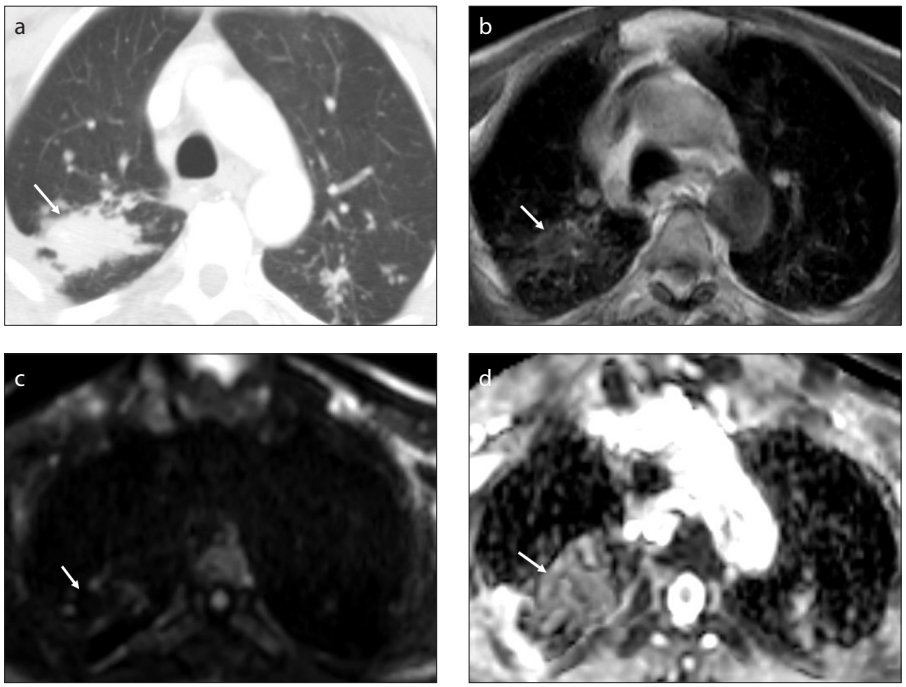

Figure 2. a–d. A 64-year-old man with PMF who worked in coal mines for 20 years. Axial contrast-enhanced computed tomography image **(a)** shows an ill-defined mass *(arrow)*. Axial T1-weighted SE image **(b)** shows an isointense lesion *(arrow)*. There is no marked diffusion restriction *(arrow)* on DWI (**c,** *arrow*). The lesion has a mildly hyperintense appearance *(arrow)* with an ADC value of 1.2 on the ADC map of DWI **(d)**.

The duration of working history in coal mines of the patient was significantly higher in our patients with PMF which could be expected as a natural finding. We also found that there was no difference between the groups in terms of age and lesion size, suggesting that both diseases can occur at similar ages and the lesions can be similar in size in both disease groups.

PMF lesions can occasionally mimic lung cancer on CT and even ^{18}F-FDG PET/CT (1, 6). Although Choi et al. (11) reported the sensitivity, specificity, and accuracy for diagnosis of lung cancer in pneumoconiosis patients as 81.0%, 73.2%, and 77.1%, respectively, with a maximum standardized uptake value (SUVmax) cutoff value of 7.4, a wide range (1.9–14.3) of SUVmax has been reported for PMF in the literature, with a mean value of 6.3 (12, 13). Morphological and functional similarities of the PMF and cancer lesions on these imaging modalities decrease their diagnostic abilities in differentiation of PMF from cancer lesions. Also, as these patients need to undergo imaging modalities periodically, repetitive exposure to ionizing radiation needs to be avoided. Another disadvantage of CT is the use of contrast agents, which can deteriorate renal functions in some patients and have allergy risk. On the other hand, MRI is very effective in the detection of lesion structure, and even unenhanced MRI sequences have high contrast resolution to demonstrate the lesion. Detailed visualization of the lesion structure is also important for a possible biopsy targeting the part that is most suspicious for cancer. Compared with ^{18}F-FDG PET/CT, an unenhanced, free-breathing MRI is a comfortable examination that has lower cost, no ionizing radiation, and no need for specific preparation before the examination. Thus, the use of MRI has been extended to include new MRI protocols aimed at differentiating PMF from lung cancer.

DWI and ADC values obtained from ADC maps have been effectively used in the diagnosis of lung cancers, since cancer lesions generally restrict diffusion due to hypercellularity (14–16). DWI and ADC values are helpful in differentiation between benign and malignant lung lesions, correlation with the grade of cancer, and in the follow-up of tumors (15–18). In the previous

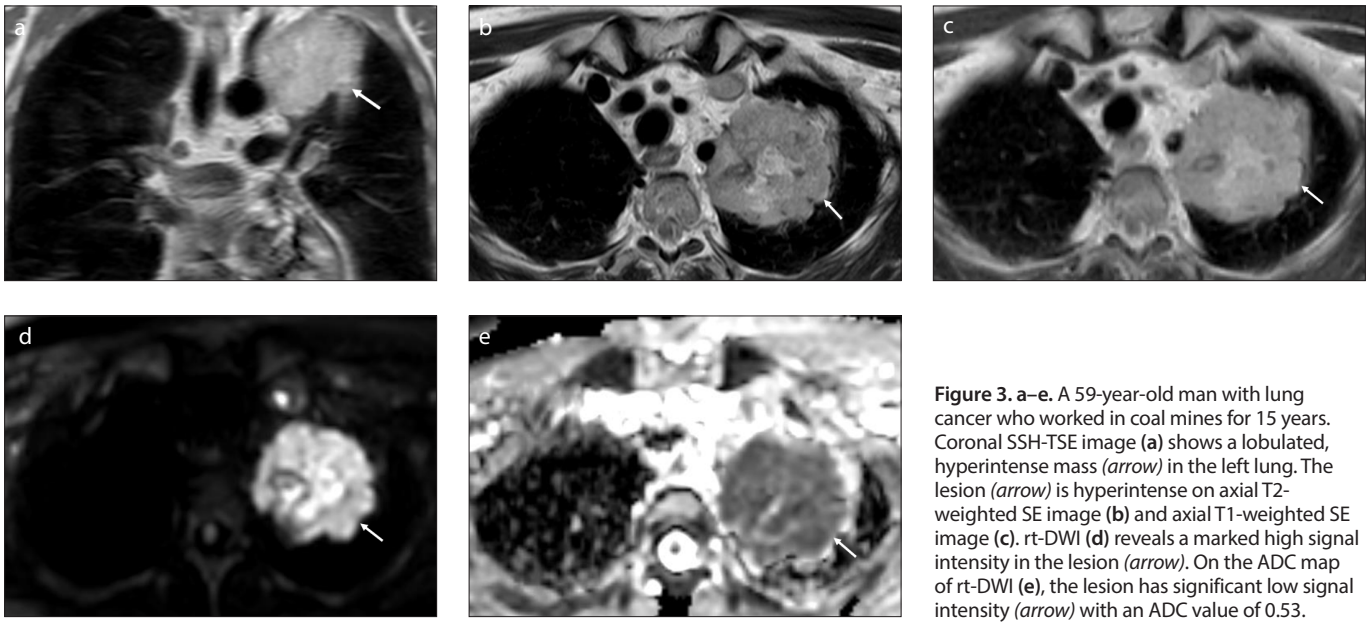

Figure 3. a–e. A 59-year-old man with lung cancer who worked in coal mines for 15 years. Coronal SSH-TSE image **(a)** shows a lobulated, hyperintense mass *(arrow)* in the left lung. The lesion *(arrow)* is hyperintense on axial T2-weighted SE image **(b)** and axial T1-weighted SE image **(c)**. rt-DWI **(d)** reveals a marked high signal intensity in the lesion *(arrow)*. On the ADC map of rt-DWI **(e)**, the lesion has significant low signal intensity *(arrow)* with an ADC value of 0.53.

studies, ROIs were placed within the solid parts of the tumor or the whole tumor to measure the ADC values (18–20). We placed ROIs within the solid and most hypointense parts of the lesions on ADC map and used a ROI of 1.5 cm^2. Due to hypercellularity of the neoplasms, most cancer lesions in our study were hyperintense on DWI and had lower ADC values compared with PMF lesions. Probably due to our assessment method, the ADC values of our patients with cancer were found to be lower than those found in the previous studies (18, 20).

DWI techniques in thorax MRI include breath-hold, free-breathing DWI, and rt-DWI. In several DWI studies of lung cancer, rt-DWI has been the most used technique due to concerns about free-breathing DWI being less accurate in the assessment of ADC values (15, 16). However, Cui et al. (19) stated that there was no significant difference between the three DWI techniques in terms of inter- and intra-observer agreement of ADC measurements in patients with lung cancer. Similarly, there was no significant difference between free-breathing DWI and rt-DWI in 57 lung adenocarcinoma lesions in terms of ADC measurements, repeatability of ADC measurements, and interobserver agreement (20). Similarly, our results confirmed that rt-DWI has no superiority to free-breathing DWI, and both free-breathing DWI and rt-DWI could be used in differentiation between PMF and cancer. A strong interobserver agreement in the assessment of ADC values was present in our study. An additional benefit of free-breathing DWI technique is the shorter time it takes compared with the application of rt-DWI. Free-breathing DWI took approximately 2.5 minutes, while rt-DWI took approximately 6 minutes in our study.

Among the qualitative MRI sequences, T1- and T2-weighted MRI play an important role in differentiation of these disease groups, since PMF lesions typically appear as hypointense on both sequences due to fibrosis (9, 21). Lung cancer generally tends to show higher SI compared with PMF lesions, particularly on T2-weighted imaging (1). In a pneumoconiosis study, Hekimoglu et al. (6) reported that homogeneous low SI was the most frequent SI type seen in 91% of patients (20 of 22) on half-Fourier single-shot turbo spin echo (HASTE) sequence. In line with this study, Ogihara et al. (1) reported that T2-weighted fast SE MRI is the most useful sequence to detect fibrosis and thus to differentiate PMF and cancer due to differences in SI. Different from these studies, we also obtained DWI and SE imaging in addition to T2-weighted TSE imaging. Most lesions in our patients with PMF (27 of 30 patients, 90%) demonstrated iso- or hypointense appearances on T2-weighted SE imaging due to the SI of fibrosis. T2-weighted SE imaging was found to be more sensitive in our study compared with SSH-TSE and BTFE in differentiation between PMF and lung cancer, since fewer patients with PMF showed predominantly iso- or hypointense SI on SSH-TSE (n=21) and BTFE (n=25). Due to a greater number of lesions demonstrating iso- or hypointense appearances on T2-weighted SE imaging, SE imaging was found to be more effective in differentiation between these diseases compared with fast SE imaging. In contrast with the study of Hekimoglu et al. (6), which had no PMF lesion with high SI on T2-weighted imaging, we had 3 PMF lesions presenting with high SI on T2-weighted SE imaging. This high SI may be due to the presence of inflammation added to the fibrosis (1).

Regarding T1-weighted imaging, Hekimoglu et al. (6) reported that in PMF patients, 16 of 22 (72%) lesions were homogeneous isointense and 2 of 22 (9%) lesions were homogeneous hypointense on pre-contrast volumetric interpolated breath-hold examination (VIBE) images, while 2 of 22 (9%) lesions showed high SI at the rim on VIBE images. In contrast, we did not demonstrate any lesions with high SI at the rim and all PMF lesions in our study showed predominantly iso- or hypointense SI on T1-weighted SE imaging. Only 6 patients with PMF had lesions showing predominantly iso- or hypointense SI on THRIVE sequence in our study. Additionally, two patients had lesions seen predominantly as iso- or hypointense on T1-weighted SE imaging in our cancer group. Unlike other studies, T1-weighted SE imaging was found to be the most valuable sequence in differentiation between PMF and lung cancer among our qualitative sequences due to

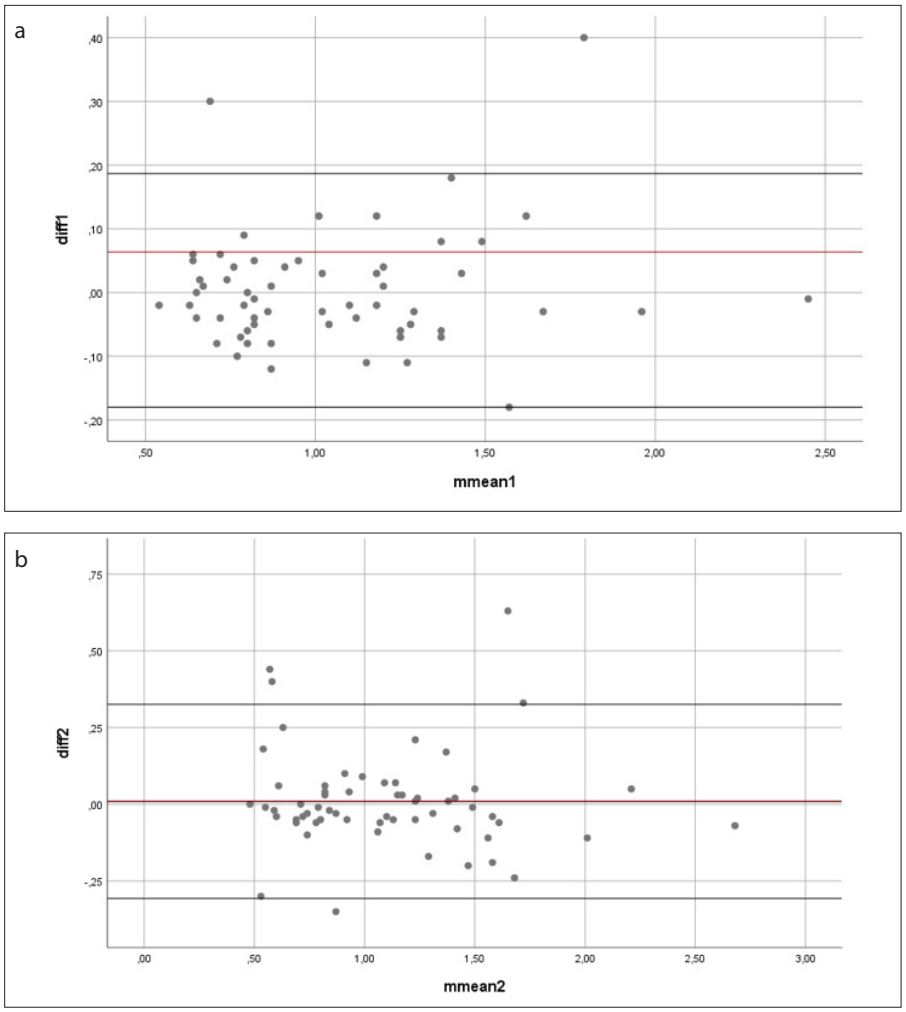

Figure 4. a, b. Visual inspection of Bland–Altman plot. Chart **(a)** shows the ADC measurements of Reader 1 and Reader 2. The longitudinal axis shows the differences in the measurements of the readers, and the horizontal axis shows the means of the measurements of the readers. Chart **(b)** shows the ADC measurements of rt-DWI of Reader 1 and Reader 2. The longitudinal axis shows the differences in the measurements of the readers, and the horizontal axis shows the means of the measurements of the readers.

iso- or hypointense SI of all 30 lesions. Considering the significant results we obtained with qualitative MRI sequences, we believe that SE sequences are superior over fast SE sequences in differentiation between PMF and lung cancer.

Contrast enhancement pattern has low sensitivity and specificity in distinguishing PMF from lung cancer (1). The diagnostic utility of enhancement pattern is less useful compared with T1- and T2-weighted MRI (1). A clear and progressive increase in SI was reported in a dynamic study with PMF patients (10). However, only 6 of 16 (38%) PMF lesions showed a progressively increased enhancement in the study of Ogihara et al. (1). This difference between the two studies might be because MRI was not performed in some patients with PMF in the study of Jung et al. (10). Additionally, lung cancers were reported to show a faster enhancement pattern compared with benign lesions on dynamic MRI studies (22). It was stated that the contrast-enhanced VIBE sequence which showed superior visualization of PMF lesions has better agreement with CT findings compared to HASTE and unenhanced VIBE sequences (6). It was also found that PMF lesions show diffuse enhancement in 12 of 22 patients (55%) and rim enhancement in 10 of 22 patients (45%) (6). We preferred not to obtain contrast-enhanced MRI in our study, since its addition to an unenhanced MRI study provides limited information in this issue and increases the duration of the study. In this way, we also avoided invasive procedures and possible complications of contrast agents in these patients.

Our study has several limitations. First, only selected PMF patients, the ones who had suspicious lesions for cancer underwent MRI, which might slightly affect our findings. Second, this was a retrospective study with a relatively small sample size. Third, a neoplasm can develop in the background of PMF lesion or as a part of it, so both diseases might be seen together. Biopsy areas should be appropriate to reach adequate diagnosis, and the radiologists can point at more adequate areas for biopsy with the help of MRI. We assessed ADC values from radiologically solid parts of the lesions to minimize this possible negative effect in our study. Additionally, contrast-enhanced MRI was not performed. Lastly, the interpretation of SI of the lesions on qualitative MRI sequences could be regarded as relatively subjective. However, we think that a fair interobserver agreement can overcome this limitation.

In conclusion, we identified several MRI-derived parameters correlating between PMF and lung cancer groups. ADC values of DWI and rt-DWI quantitatively and the SIs on MRI sequences, such as T1-, T2-weighted SE, and SSH-TSE qualitatively were found to be strong predictors in differentiation between PMF and lung cancer. T1-weighted SE imaging was demonstrated as the most significant sequence in qualitative interpretation in our study. A noninvasive, tolerable, and multiparametric MRI examination including SE imaging and ADC values of DWI may increase the diagnostic ability and contribute to distinguishing PMF from lung cancer. Future studies are required to further explore the potential added value of MRI in the differentiation of these diseases.

Conflict of interest disclosure

The authors declared no conflicts of interest.

References

1. Ogihara Y, Ashizawa K, Hayashi H, et al. Progressive massive fibrosis in patients with pneumoconiosis: utility of MRI in differentiating from lung cancer. Acta Radiol 2018; 59:72–80. [Crossref]
2. Chong S, Lee KS, Chung MJ, Han J, Han J, Kwon OJ, Kim TS. Pneumoconiosis: comparison of imaging and pathologic findings. Radiographics 2006; 26:59–77. [Crossref]
3. Soutar CA, Collins HP. Classification of progressive massive fibrosis of coalminers by type of radiographic appearance. Br J Ind Med 1984; 41:334–339. [Crossref]

4. Remy-Jardin M, Degreef JM, Beuscart R, Voisin C, Remy J. Coal worker's pneumoconiosis: CT assessment in exposed workers and correlation with radiographic findings. Radiology 1990; 177:363–371. [Crossref]
5. Bergin CJ, Muller NL, Vedal S, Chan-Yeung M. CT in silicosis: correlation with plain films and pulmonary function tests. AJR Am J Roentgenol 1986; 146:477–483. [Crossref]
6. Hekimoglu K, Sancak T, Tor M, Besir H, Kalaycioglu B, Gundogdu S. Fast MRI evaluation of pulmonary progressive massive fibrosis with VIBE and HASTE sequences: comparison with CT. Diagn Interv Radiol 2010; 16:30–37. [Crossref]
7. Dholakia S, Rappaport DC. The solitary pulmonary nodule. Is it malignant or benign? Postgrad Med 1996; 99:246–250.
8. Viggiano RW, Swensen SJ, Rosenow EC 3rd. Evaluation of management of solitary and multiple pulmonary nodules. Clin Chest Med 1992; 13:83–95.
9. Matsumoto S, Mori H, Miyake H, et al. MRI signal characteristics of progressive massive fibrosis in silicosis. Clin Radiol 1998; 53:510–514. [Crossref]
10. Jung JI, Park SH, Lee JM, Hahn ST, Kim KA. MR characteristics of progressive massive fibrosis. J Thorac Imaging 2000; 15:144–150. [Crossref]
11. Choi EK, Park HL, Yoo IR, Kim SJ, Kim YK. The clinical value of F-18 FDG PET/CT in differentiating malignant from benign lesions in pneumoconiosis patients. Eur Radiol 2020; 30:442–451. [Crossref]
12. Reichert M, Bensadoun ES. PET imaging in patients with coal workers pneumoconiosis and suspected malignancy. J Thorac Oncol 2009; 4:649–651. [Crossref]
13. Kanegae K, Nakano I, Kimura K, et al. Comparison of MET-PET and FDG-PET for differentiation between benign lesions and lung cancer in pneumoconiosis. Ann Nucl Med 2007; 21:331–337. [Crossref]
14. Charles-Edwards EM, deSouza NM. Diffusion-weighted magnetic resonance imaging and its application to cancer. Cancer Imaging 2006; 6:135–143. [Crossref]
15. Reischauer C, Froehlich JM, Pless M, Binkert CA, Koh DM, Gutzeit A. Early treatment response in non-small cell lung cancer patients using diffusion-weighted imaging and functional diffusion maps--a feasibility study. PLoS One 2014; 9:e108052. [Crossref]
16. Yu J, Li W, Zhang Z, Yu T, Yu T, Li D. Prediction of early response to chemotherapy in lung cancer by using diffusion-weighted MR imaging. Scientific World Journal 2014; 2014:135841. [Crossref]
17. Liu H, Liu Y, Yu T, Ye N. Usefulness of diffusion-weighted MR imaging in the evaluation of pulmonary lesions. Eur Radiol 2010; 20:807–815. [Crossref]
18. Liu H, Liu Y, Yu T, Ye N, Wang Q. Evaluation of apparent diffusion coefficient associated with pathological grade of lung carcinoma, before therapy. J Magn Reson Imaging 2015; 42:595–601. [Crossref]
19. Cui L, Yin JB, Hu CH, Gong SC, Xu JF, Yang JS. Inter- and intraobserver agreement of ADC measurements of lung cancer in free breathing, breath-hold and respiratory triggered diffusion-weighted MRI. Clin Imaging 2016; 40:892–896. [Crossref]
20. Swerkersson S, Grundberg O, Kolbeck K, Carlberg A, Nyrén S, Skorpil M. Optimizing diffusion-weighted magnetic resonance imaging for evaluation of lung tumors: A comparison of respiratory triggered and free breathing techniques. Eur J Radiol Open 2018; 5:189–193. [Crossref]
21. Matsumoto S, Miyake H, Oga M, Takaki H, Mori H. Diagnosis of lung cancer in a patient with pneumoconiosis and progressive massive fibrosis using MRI. Eur Radiol 1998; 8:615–617. [Crossref]
22. Fujimoto K. Usefulness of contrast-enhanced magnetic resonance imaging for evaluating solitary pulmonary nodules. Cancer Imaging 2008; 8:34–44. [Crossref]